Developmental Cell, Volume *51*

Supplemental Information

Reconstruction of the Global Neural Crest Gene Regulatory Network *In Vivo*

Ruth M. Williams, Ivan Candido-Ferreira, Emmanouela Repapi, Daria Gavriouchkina, Upeka Senanayake, Irving T.C. Ling, Jelena Telenius, Stephen Taylor, Jim Hughes, and Tatjana Sauka-Spengler

Reconstruction of the global neural crest gene regulatory network *in vivo*

Ruth M Williams[1], Ivan Candido-Ferreira[1], Emmanouela Repapi[2], Daria Gavriouchkina[1,5], Upeka Senanayake[1], Irving T C Ling[1,4], Jelena Telenius[2,3], Stephen Taylor[2], Jim Hughes[2,3], and Tatjana Sauka-Spengler[1,*]

Supplemental Material

---

*Lead and corresponding author: Tatjana Sauka-Spengler (tatjana.sauka-spengler@imm.ox.ac.uk)
[1]University of Oxford, MRC Weatherall Institute of Molecular Medicine, Radcliffe Department of Medicine, Oxford, OX3 9DS, UK
[2]University of Oxford, MRC Centre for Computational Biology, Weatherall Institute of Molecular Medicine, Oxford, OX3 9DS, UK
[3]University of Oxford, MRC Molecular Haematology Unit, Weatherall Institute of Molecular Medicine, Oxford, OX3 9DS, UK
[4]University of Oxford, Department of Paediatric Surgery, Childrens Hospital Oxford, Oxford, UK
[5]Present Address: Okinawa Institute of Science and Technology, Molecular Genetics Unit, Onna, 904-0495, Japan

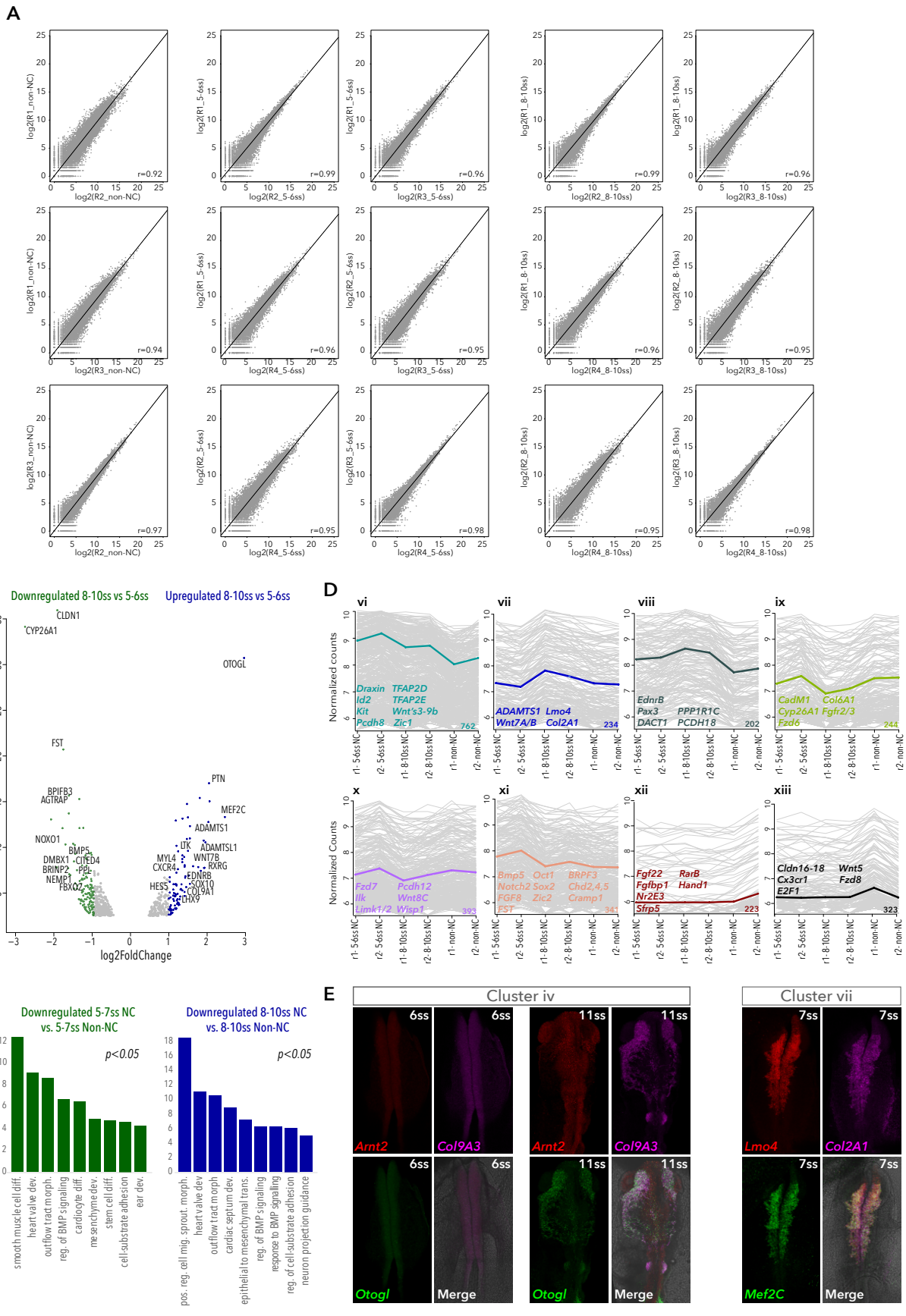
A
B
Downregulated 8-10ss vs 5-6ss
Upregulated 8-10ss vs 5-6ss
CLDN1
CYP26A1
OTOGL
FST
PTN
BPIFB3
AGTRAP
MEF2C
ADAMTS1
NOXO1
LIK
ADAMTSL1
BMP5
CITED4
DMBX1
MYL4
WNT7B
BRINP2
CXCR4
RXRG
PBL
NEMP1
EDNRB
FBXO2
HES5
SOX10
COL9A1
CHX9
−log10(padj)
log2FoldChange
C
Downregulated 5-7ss NC
vs. 5-7ss Non-NC
p<0.05
Downregulated 8-10ss NC
vs. 8-10ss Non-NC
p<0.05
Fold enrichment
smooth muscle cell diff.
heart valve dev.
outflow tract morph.
reg. of BMP signaling
cardiocyte diff.
mesenchyme dev.
stem cell diff.
cell-substrate adhesion
ear dev.
pos. reg. cell mig.
sprout. morph.
heart valve dev
outflow tract morph
cardiac septum dev.
epithelial to mesenchymal trans.
reg. of BMP signaling
response to BMP signaling
reg. of cell-substrate adhesion
neuron projection guidance
D
vi
vii
viii
ix
x
xi
xii
xiii
Normalized counts
Normalized Counts
Draxin TFAP2D
Id2 TFAP2E
Kit Wnt's-9b
Pcdh8 Zic1
762
ADAMTS1 Lmo4
Wnt7A/B Col2A1
234
EdnrB
Pax3 PPP1R1C
DACT1 PCDH18
202
CadM1 Col6A1
Cyp26A1 Fgfr2/3
Fzd6
244
Fzd7 Pcdh12
Ilk Wnt8C
Limk1/2 Wisp1
393
Bmp5 Oct1 BRPF3
Notch2 Sox2 Chd2,4,5
FGF8 Zic2 Cramp1
FST
341
Fgf22 RarB
Fgfbp1 Hand1
Nr2E3
Sfrp5
223
Cldn16-18 Wnt5
Cx3cr1 Fzd8
E2F1
323
r1- 5-6ss NC
r2- 5-6ss NC
r1- 8-10ss NC
r2- 8-10ss NC
r1- non-NC
r2- non-NC
E
Cluster iv
Cluster vii
6ss
11ss
7ss
Arnt2
Col9A3
Otogl
Merge
Lmo4
Col2A1
Mef2C

Figure S1. RNA-seq quality control and reproducibility. Related to figure 1 (A) Scatter plots showing correlation of RNA-seq replicas. r= Pearson correlation co-efficient. **(B)** Volcano plot of genes enriched and depleted at 8-10ss compared to 5-6ss. Differential expression analysis was performed using DESeq2 with a negative binomial model, *p*-values were calculated using Wald test, with Benjamin-Hochberg correction for multiple testing (*p*-adjusted, padj.). **(C)** Gene ontology terms associated with genes depleted in NC compared to non-NC cells at 5-6ss and 8-10ss (LogFoldChange<-1, *padj*<0.05, base mean>50) . Enriched GO terms were obtained using statistical overrepresentation test, *p*-values were calculated with binomial distributions and Bonferroni correction for multiple hypothesis testing. **(D)** Clusters (vi-xiii) of highly correlated genes identified by WGCNA. **(E)** Co-localisation of gene expression for selected genes from cluster-iv and vii obtained using HCR (Hybridisation Chain Reaction).

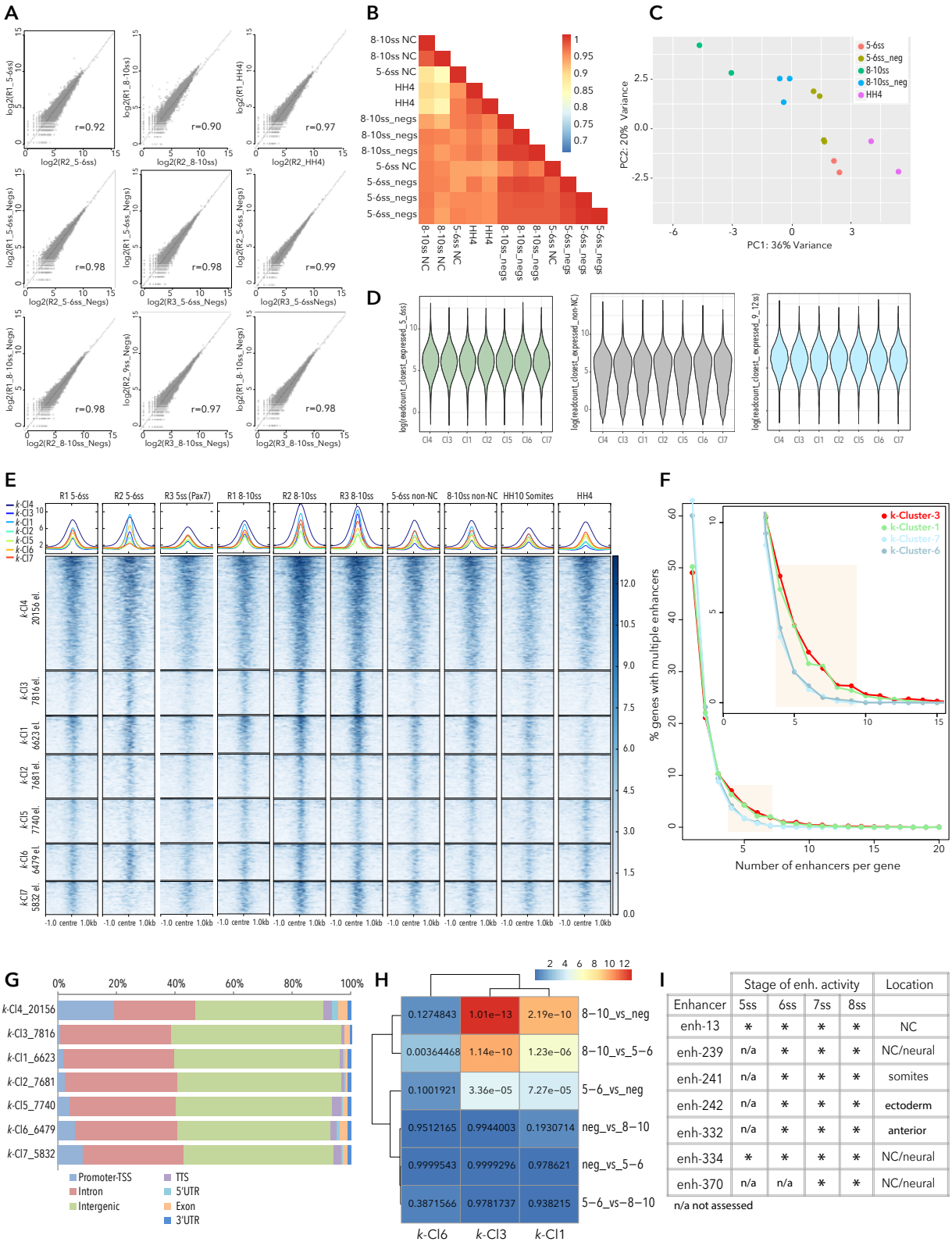

	Stage of enh. activity				Location
Enhancer	5ss	6ss	7ss	8ss	
enh-13	*	*	*	*	NC
enh-239	n/a	*	*	*	NC/neural
enh-241	n/a	*	*	*	somites
enh-242	n/a	*	*	*	ectoderm
enh-332	n/a	*	*	*	anterior
enh-334	*	*	*	*	NC/neural
enh-370	n/a	n/a	*	*	NC/neural

n/a not assessed

Figure S2. ATAC-seq quality control and chromatin accessibility dynamics. Related to Figures 2 and 3. (A) Scatter plots showing correlation of ATAC-seq replicas, r= Pearson correlation co-efficient. **(B)** Matrix presenting the Pearson correlation coefficients to all possible pairwise comparisons of replicates/samples. **(C)** PCA comparing NC and non-NC cells at both stages and HH4 ATAC-seq samples. **(D)** Violin plots showing correlation between *k*-Cluster elements and gene expression levels. **(E)** Heatmap and merged profiles depicting *k*-means linear enrichment clustering of ATAC signal across all samples/stages analysed. Pax7 sample is NC cells isolated using the *Pax7* enh-195 (Figure S3D). **(F)** Percentage of genes with multiple associated enhancers. **(G)** Stacked bar plot showing genomic annotation of *k*-Cluster elements. The number of elements in each *k*-Cluster is also shown. **(H)** Heatmap represents statistical significance of the associations of differentially expressed genes as per bulk RNA-seq analysis and selected *k*-means clusters calculated as overrepresentation of enriched/depleted genes within the sets of genes regulated by the given *k*-means cluster. *P*-values, calculated using two-tailed hypergeometric test, are shown in the corresponding positions within the heatmap. Colour bar corresponds to -log(*p*-values). **(I)** Table summarising spatio-temporal *Snai2* enhancer activity.

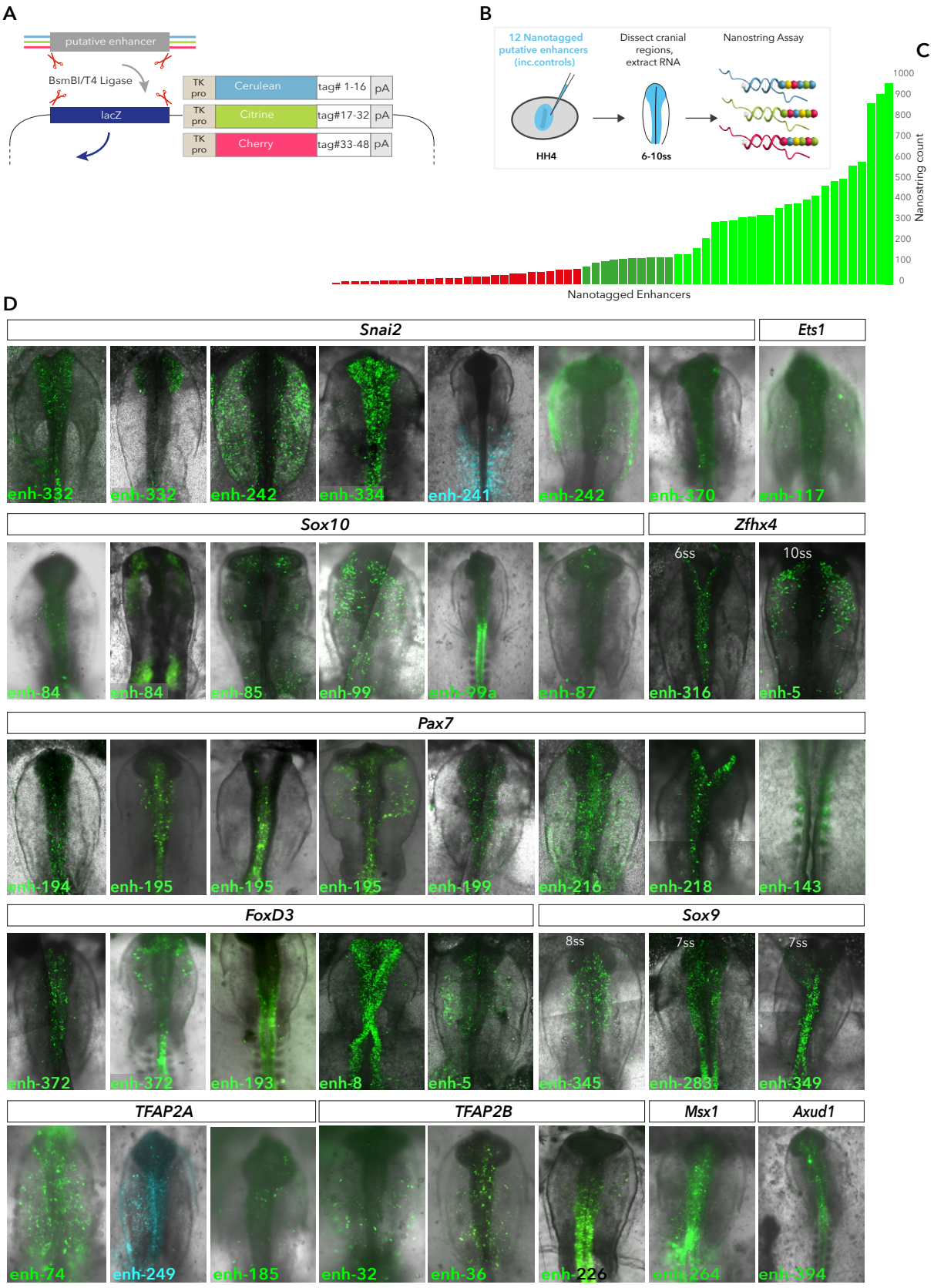
A
putative enhancer
BsmBI/T4 Ligase
lacZ
TK pro
Cerulean
tag# 1-16
pA
TK pro
Citrine
tag#17-32
pA
TK pro
Cherry
tag#33-48
pA
B
12 Nanotagged putative enhancers (inc.controls)
Dissect cranial regions, extract RNA
Nanostring Assay
HH4
6-10ss
C
Nanostring count
1000
900
800
700
600
500
400
300
200
100
0
Nanotagged Enhancers
D
Snai2
Ets1
enh-332
enh-332
enh-242
enh-334
enh-241
enh-242
enh-370
enh-117
Sox10
Zfhx4
enh-84
enh-84
enh-85
enh-99
enh-99a
enh-87
6ss
enh-316
10ss
enh-5
Pax7
enh-194
enh-195
enh-195
enh-195
enh-199
enh-216
enh-218
enh-143
FoxD3
Sox9
enh-372
enh-372
enh-193
enh-8
enh-5
8ss
enh-345
7ss
enh-288
7ss
enh-349
TFAP2A
TFAP2B
Msx1
Axud1
enh-74
enh-249
enh-185
enh-32
enh-36
enh-226
enh-264
enh-394

Figure S3. Multiplexed high-throughput enhancer screening. Related to Figures 3 and 4. (A) Schematic depiction of enhancer cloning strategy. **(B)** Cartoon showing *ex ovo* electroporation technique and Nanostring assay. **(C)** Bar graph representing typical Nanostring results. Nanostring count (of nanotag transcripts) above 50 (green) was determined to reflect *in vivo* enhancer activity. **(D)** *In vivo* activity of selected enhancers. Imaging was performed using either fluorescent stereo microscope or confocal microscopy. In the latter case, embryo z-stack scans were collected across approximately 50-70 μm, and horizontal tiling was used to image the entire embryo at high magnification. In such cases, images were processed using bidirectional stitching mode of the Zeiss Zen microscope software with 10% overlap. For confocal images, the maximum intensity projection of a z-stack is shown.

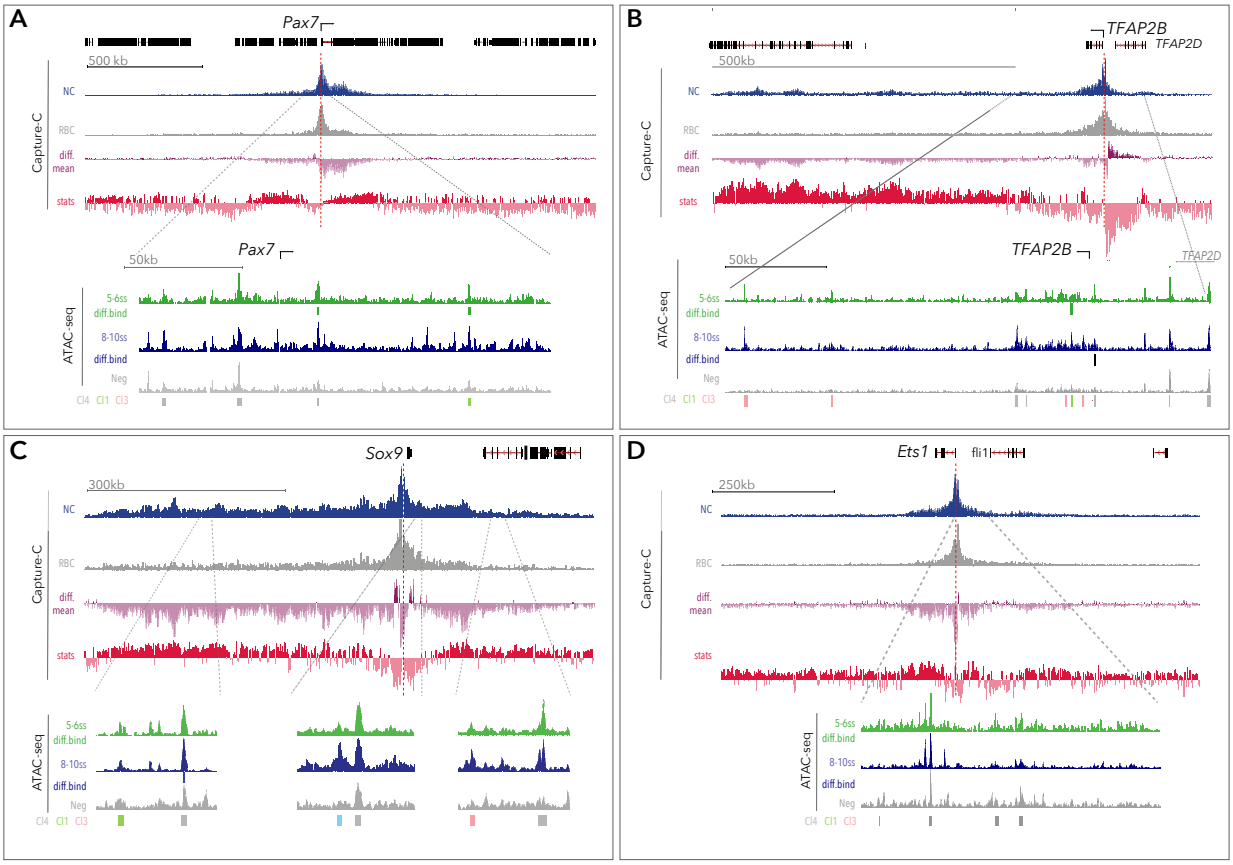
A
Pax7
500 kb
Capture-C
NC
RBC
diff. mean
stats
50kb
ATAC-seq
5-6ss diff.bind
8-10ss diff.bind
Neg
Cl4 Cl1 Cl3
B
TFAP2B
TFAP2D
500kb
50kb
C
Sox9
300kb
D
Ets1
fli1
250kb

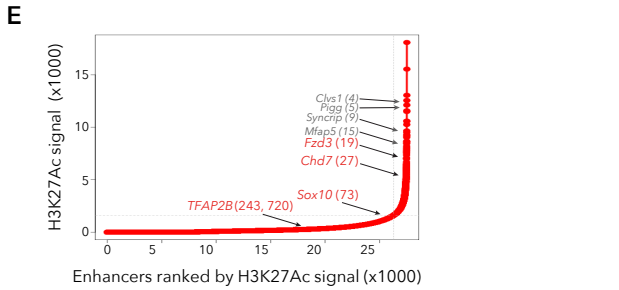
E
H3K27Ac signal (x1000)
Clvs1 (4)
Pigg (5)
Syncrip (9)
Mfap5 (15)
Fzd3 (19)
Chd7 (27)
Sox10 (73)
TFAP2B (243, 720)
Enhancers ranked by H3K27Ac signal (x1000)

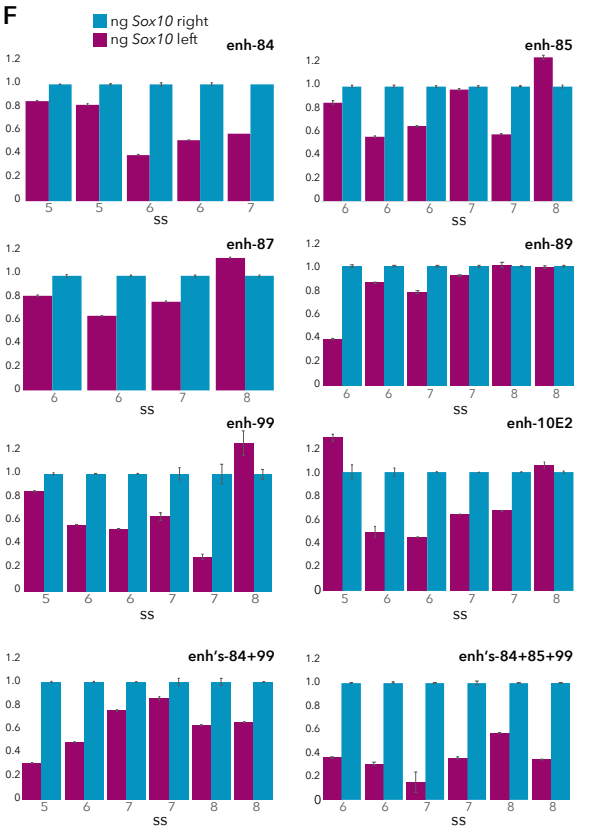
F
ng Sox10 right
ng Sox10 left
enh-84
enh-85
enh-87
enh-89
enh-99
enh-10E2
enh's-84+99
enh's-84+85+99
SS

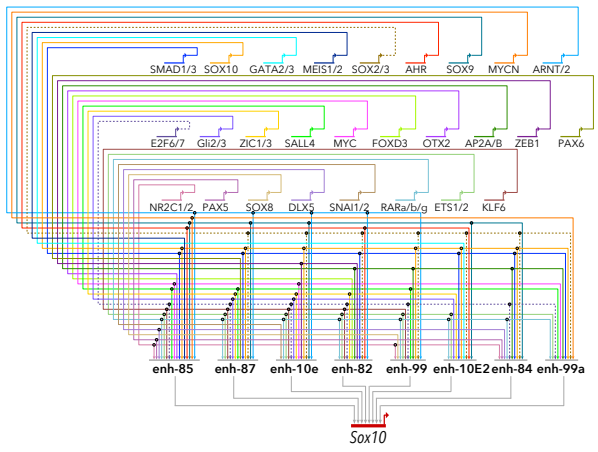
G
SMAD1/3 SOX10 GATA2/3 MEIS1/2 SOX2/3 AHR SOX9 MYCN ARNT/2
E2F6/7 Gli2/3 ZIC1/3 SALL4 MYC FOXD3 OTX2 AP2A/B ZEB1 PAX6
NR2C1/2 PAX5 SOX8 DLX5 SNAI1/2 RARa/b/g ETS1/2 KLF6
enh-85 enh-87 enh-10e enh-82 enh-99 enh-10E2 enh-84 enh-99a
Sox10

Figure S4. Capture-C at NC loci and decommissioning super-enhancer elements controlling *Sox10* expression. Related to Figures 3 and 4. Genome browser views of chromosome conformation capture from the *Pax7* **(A)**, *TFAP2B* ***(B)***, *Sox9* **(C)** and *Ets1* **(D)** promoters (Capture-C) and associated statistical analysis of the differences between Capture-C profiles in NC and RBC (n=4 each). Raw counts of unique interactions mapped to each restriction fragment were analysed using the bioconductor package DESeq2. The red dashed line denotes the position of the capture probe. Tracks show the Capture-C normalised counts from raw count per restriction fragment from NC cells (blue) and RBCs (grey), respectively. The differential mean track (purple) specifically highlights proximal and distal interaction blocks, with NC-specific interactions overlapping distal *cis*-regulatory elements (ATAC-seq tracks and mapped analysed *k*-Cluster and Diffbind elements). The majority of differences are with elements that interact more strongly in NC than in RBCs and the DESeq2 analysis highlighted these interactions as being statistically significant. Statistical significance is presented in the form of the DEseq2 Wald statistics track (stat, in red), which determines significance of difference in interactions between NC and RBCs, and is calculated as a ratio of LogFoldChange values and their standard errors, determined using DESeq2, *p*-values calculated with Wald test and Benjamin-Hochberg correction. This indicates the significant differences between NC and RBC profiles, and points to both proximal and distal interactions. **(E)** Enhancers ranked by H3K27ac signal from 5-6ss, using the ROSE algorithm, top-ranked genes are annotated. **(F)** qPCR for *Sox10* following dCas9-Krab mediated decommissioning of associated enhancers using bilateral electroporation (Fig. 4K-N). *Sox10* on the left (experimental) side of embryos shown in magenta, right (control) side shown in blue. Error bars show standard deviation. **(G)** *Sox10* gene regulatory sub-circuit inferred from known vertebrate TF binding models. Interactions via five novel enhancers (enh-82, enh-84, enh-85, enh-87, enh-99) and published 10E and 10E2 enhancer are shown. Dashed lines represent possible repressive interactions

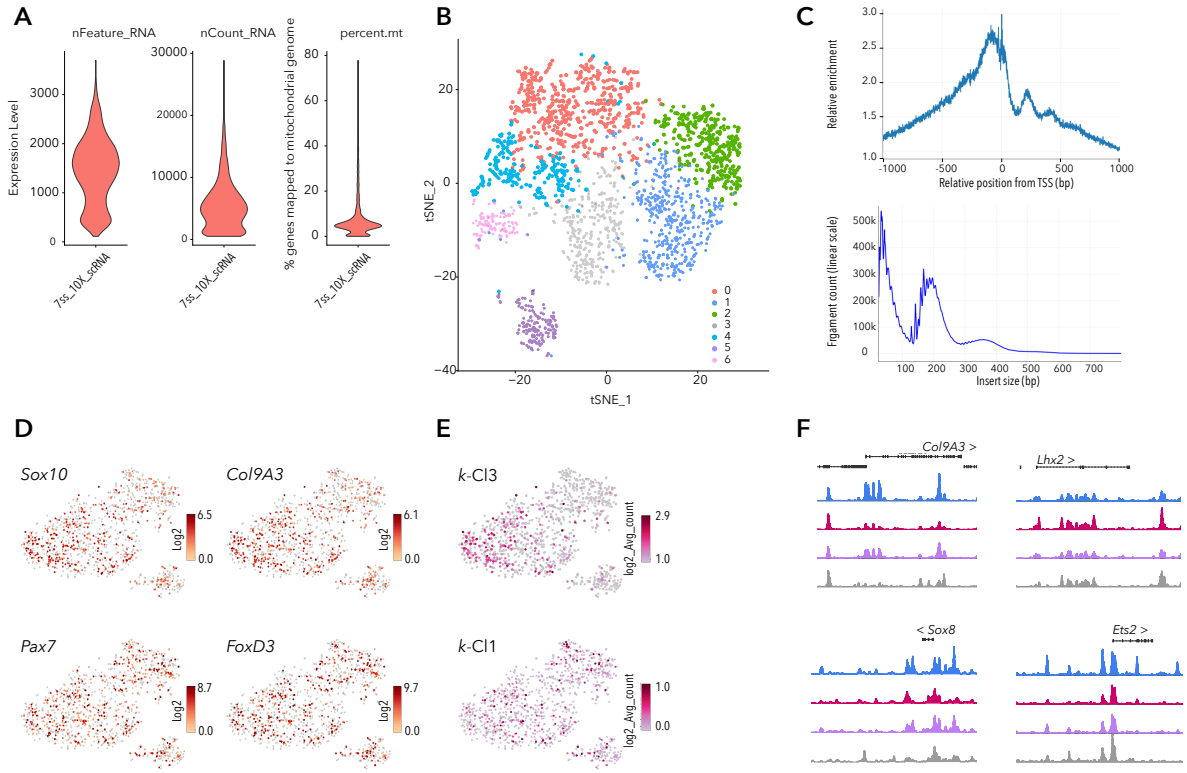
A
nFeature_RNA
nCount_RNA
percent.mt
Expression Level
% genes mapped to mitochondrial genome
7ss_10X_scRNA
B
tSNE_1
tSNE_2
C
Relative enrichment
Relative position from TSS (bp)
Frgament count (linear scale)
Insert size (bp)
D
Sox10
Col9A3
Pax7
FoxD3
Log2
E
k-Cl3
k-Cl1
log2_Avg_count
F
Col9A3 >
Lhx2 >
< Sox8
Ets2 >

Figure S5. Quality control of scRNA and scATAC experiments. Related to Figure 5. **(A)** Violin plots showing distribution of nFeatures, nCounts and reads mapped to mitochondrial genome. Features were filtered to include >200 and <3000, counts filtered to <10000 and mitochondrial reads <10%. **(B)** tSNE of all 7 10X Chromium scRNA-seq clusters. **(C)** Distribution and size of scATAC peaks. **(D)** tSNEs highlighting NC genes across scATAC clusters. **(E)** tSNE plots showing localisation of *k*-Clusters across scATAC clusters. **(F)** scATAC profiles at selected NC gene loci.

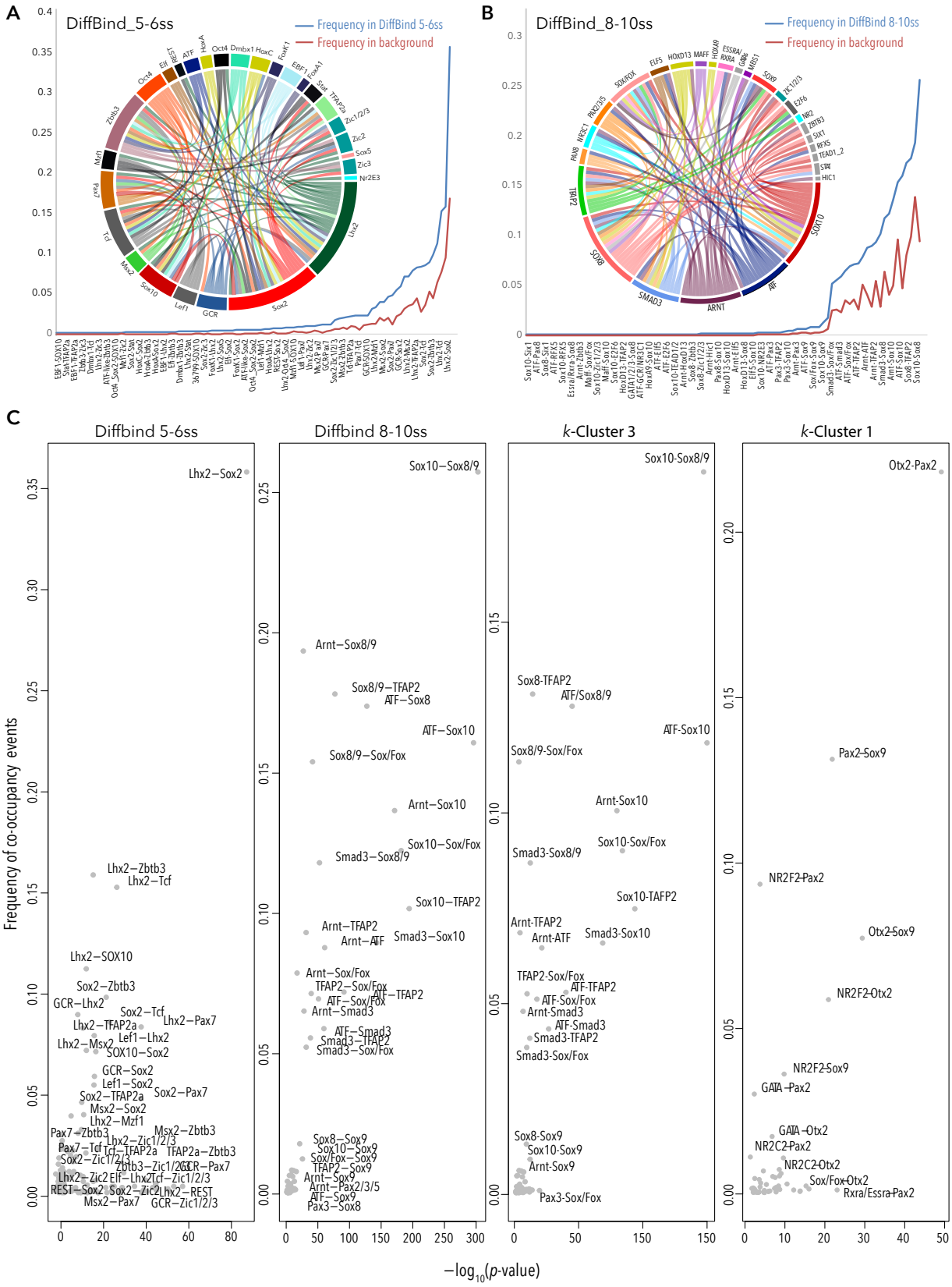
A
DiffBind_5-6ss
Frequency in DiffBind 5-6ss
Frequency in background
B
DiffBind_8-10ss
Frequency in DiffBind 8-10ss
Frequency in background
C
Diffbind 5-6ss
Diffbind 8-10ss
k-Cluster 3
k-Cluster 1
Frequency of co-occupancy events
−log10(p-value)
Lhx2−Sox2
Lhx2−Zbtb3
Lhx2−Tcf
Lhx2−SOX10
Sox2−Zbtb3
GCR−Lhx2
Sox2−Tcf
Lhx2−TFAP2a
Lhx2−Pax7
Lhx2−Msx2
Lef1−Lhx2
SOX10−Sox2
GCR−Sox2
Lef1−Sox2
Sox2−TFAP2a
Sox2−Pax7
Msx2−Sox2
Lhx2−Mzf1
Pax7−Zbtb3
Msx2−Zbtb3
Lhx2−Zic1/2/3
Pax7−Tcf
Tcf−TFAP2a
TFAP2a−Zbtb3
Sox2−Zic1/2/3
Zbtb3−Zic1/2/3
GCR−Pax7
Lhx2−Zic2
Elf−Lhx2
Tcf−Zic1/2/3
REST−Sox2
Sox2−Zic2
Lhx2−REST
Msx2−Pax7
GCR−Zic1/2/3
Sox10−Sox8/9
Arnt−Sox8/9
Sox8/9−TFAP2
ATF−Sox8
ATF−Sox10
Sox8/9−Sox/Fox
Arnt−Sox10
Sox10−Sox/Fox
Smad3−Sox8/9
Sox10−TFAP2
Arnt−TFAP2
Arnt−ATF
Smad3−Sox10
Arnt−Sox/Fox
TFAP2−Sox/Fox
ATF−Sox/Fox
ATF−TFAP2
Arnt−Smad3
ATF−Smad3
Smad3−TFAP2
Smad3−Sox/Fox
Sox8−Sox9
Sox10−Sox9
Sox/Fox−Sox9
TFAP2−Sox9
Arnt−Sox9
Arnt−Pax2/3/5
ATF−Sox9
Pax3−Sox8
Sox10-Sox8/9
Sox8-TFAP2
ATF/Sox8/9
ATF-Sox10
Sox8/9-Sox/Fox
Arnt-Sox10
Smad3-Sox8/9
Sox10-Sox/Fox
Sox10-TAFP2
Arnt-TFAP2
Arnt-ATF
Smad3-Sox10
TFAP2-Sox/Fox
ATF-TFAP2
ATF-Sox/Fox
Arnt-Smad3
ATF-Smad3
Smad3-TFAP2
Smad3-Sox/Fox
Sox8-Sox9
Sox10-Sox9
Arnt-Sox9
Pax3-Sox/Fox
Otx2-Pax2
Pax2-Sox9
NR2F2-Pax2
Otx2-Sox9
NR2F2-Otx2
NR2F2-Sox9
GATA-Pax2
GATA-Otx2
NR2C2-Pax2
NR2C2-Otx2
Sox/Fox-Otx2
Rxra/Essra-Pax2

Figure S6. Combinatorial transcription factor binding in DiffBind elements. Related to Figure 6. **(A, B)** Motif co-occurrence frequencies and circular spider plots showing putative TF combinatorial binding interactions in DiffBind 5-6ss **(A)** and DiffBind 8-10ss **(B)**. **(C)** Annotated scatter plots showing frequency of TF co-occupancy events and statistical significance in DiffBind 5-6ss, 8-10ss and *k*-Cluster-3 and *k*-Cluster-1. *P*-values were calculated using two-tailed Chi-squared test, with Bonferroni correction for multiple hypothesis testing.

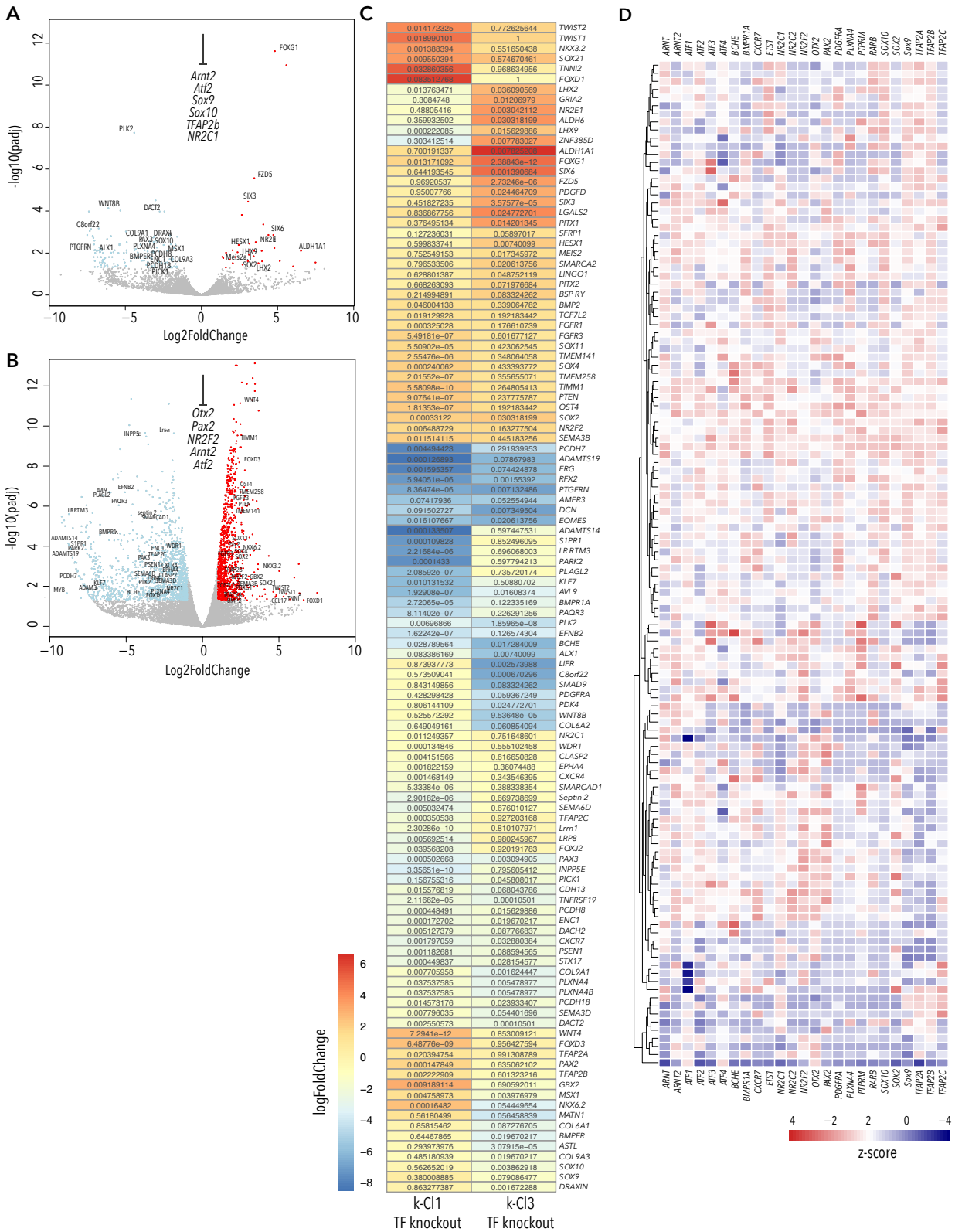
A
-log10(padj)
Log2FoldChange
Arnt2
Atf2
Sox9
Sox10
TFAP2b
NR2C1
FOXG1
PLK2
FZD5
SIX3
WNT8B
DACT2
C8orf22
SIX6
NR2E1
ALDH1A1
PTGFRN
ALX1
HESX1
LHX9
LHX2
B
-log10(padj)
Log2FoldChange
Otx2
Pax2
NR2F2
Arnt2
Atf2
WNT4
TIMM1
FOXD3
FOXD1
C
logFoldChange
k-Cl1
TF knockout
k-Cl3
TF knockout
TWIST2
TWIST1
NKX3.2
SOX21
TNNI2
FOXD1
LHX2
GRIA2
NR2E1
ALDH6
LHX9
ZNF385D
ALDH1A1
FOXG1
SIX6
FZD5
PDGFD
SIX3
LGALS2
PITX1
SFRP1
HESX1
MEIS2
SMARCA2
LINGO1
PITX2
BSPRY
BMP2
TCF7L2
FGFR1
FGFR3
SOX11
TMEM141
SOX4
TMEM258
TIMM1
PTEN
OSTN
SOX2
NR2F2
SEMA3B
PCDH7
ADAMTS19
ERG
RFX2
PTGFRN
AMER3
DCN
EOMES
ADAMTS14
S1PR1
LRRTM3
PARK2
PAQR3
PLK2
EFNB2
BMPR1A
AVL9
PLAGL2
KLF7
BCHE
ALX1
LIFR
C8orf22
SMAD9
PDGFRA
PDK4
WNT8B
COL6A2
NR2C1
WDR1
CLASP2
EPHA4
CXCR4
SMARCAD1
Septin 2
SEMA6D
TFAP2C
Lrrn1
LRP8
FOXJ2
PAX3
INPP5E
PICK1
CDH13
TNFRSF19
PCDH8
ENC1
DACH2
CXCR7
PSEN1
STX17
COL9A1
PLXNA4
PLXNA4B
PCDH18
SEMA3D
DACT2
WNT4
FOXD3
TFAP2A
PAX2
TFAP2B
GBX2
MSX1
NKX6.2
MATN1
COL6A1
BMPER
ASTL
COL9A3
SOX10
SOX9
DRAXIN
D
ARNT
ARNT2
ATF1
ATF2
ATF3
ATF4
BCHE
BMPR1A
CXCR7
ETS1
NR2C1
NR2C2
NR2F2
OTX2
PAX2
PDGFRA
PLXNA4
PTPRM
RARB
SOX10
SOX2
Sox9
TFAP2A
TFAP2B
TFAP2C
z-score

Figure S7. Perturbation of core NC-GRN transcription factors. Related to Figure 6. (A-B) Volcano plots showing misregulated genes following CRISPR knockout of core TFs associated with *k*-Cl3 **(A)** and *k*-Cl1 **(B)**. Differential expression was determined using DESeq2 with a negative binomial model, and hypothesis testing was performed with the Wald test corrected using the Benjamin-Hochberg method for multiple testing (*p*adj). Only genes with *p*adj$<$0.1 and Log2Foldchange$>$1 (in red) or Log2Foldchange$<$1 (in blue) are coloured. **(C)** Heatmap showing LogFoldChange (experimental versus control side) for a subset of differentially expressed genes following knockout of the core *k*-Cl3 factors (1st column) and the core *k*-Cl1 factors (second column). Corresponding *p*-values are annotated. **(D)** Heatmap showing single-cell co-expression of targeted core TFs and selected misregulated genes following CRISPR knockout of core TFs. Colour bar represents z-score.

Supp. table 1. Capture-C targets and oligo sequences. Related to figure 2.

Gene target	GalGal4 location	Capture oligo sequence
Sox10	chr1:50,912,325-50,912,444	TTTTCAAATCAGGGGACAGTGATGCTGTGGCAGGGACTTACAGAGGTGA CTGCAGACAGTGAGAGAGGAGGGGTGCACAGGGCAGGCAGCTCAGGTCC TGGGCTTCTCTTCAAGTTGATCGATCAAGGACATGCTGGGGATGTGGAT ACCACAAGCGTGTTGGTGGTGGCGGGGGTAAGGAAGGGGAGCTCAGCCC TGGGTTGCACAACTTCACATCCCTTCCTGTGACCAGCAACTCCA
Sox9	chr18:9,068,402-9,068,521	AGCCGGGCTGCGCGCTGGTGGAGACTCCGTCTCTGCCGGCTTTACTTCT TGTTTTTAACCCTTCCCCGCCCCTCAGCCGCCCGGTTGTTTTTTTTCTC TCCGTTTTCTCCTCCCCTGATCGATCCGCGGGAACCCCTCCGGCACGCA GCGCACGGACTTCGGCGCCTGGGAAGCCCGAAGCCGTCGCGGGGCGGAG CGAAGAGAAGCGCAACGGCTCCCACCGCCCCGCGCCCCGCCCCG
Lmo4	chr8:14,676,982-14,677,101	GCTTTTTTAATGGAGACGGAGGGAGGGACGCGCGGAGAGCTGGCAATTT GTAGGACGAAAATGGATGCTTAATTCACGTCTCGGTTTTAATTAGGTGA TTCACCGGATTTCTCCCGGATCGATCTTCCCCCCGCAGCCGGCGCACCT CTTCCACGAGAGGGAGCCCGCCGTCACCGGGGGCGGCTGCGCGCTGCCG CCGGGGTTCACCATGGCCTGCGGGAGAGCGGCGCGGGTCAGGGG
Pax7	chr21:4,443,114-4,443,233	TTTGGGGCGGTTGGAGCTCCTTTCCCACGCCGCGCCTTTCCCCGAGCAG CTGTGCCGCTTTGCTCTTTATTTCTCCTCCCGTTTCAAGTAGTGAGGAG CCGGCTTTCAGAAGCCAGGATCGATCCAATTCATTAAGGATGCTAATGA AGGAGGTGCGTCGGGAGCCGCCGAGCGCAGAGCGGAGGGGTTTGGGTCT CATTTCGGCCCTATATACGGGGGGGTGATGTGGAAGGAATGCTG
Snai2	chr2:108,126,987-108,127,106	GATCCTCTTTGAATAACTGAGTTCAAGTGGATGAACAAACTTCATGATT CATTCCGAGCAGCGCTGACATATTTGTCCGAACTGCCTCACTGTAAGCA CGGCAAAAAAACAGAGCTAGCGGGGAGAAGCGCAGCTCTTCACAGCACT GAGGGCAAAGCTGCTGCTTTCCTTCACTGTACAGAAACGATTAAATCCA CTTTTGGAAGGGACGTTCGTGACGCCGGTCGCCTCTCAGCGATC
TFAP2b	chr3:107,873,143-107,873,262	GATCCATCTATAATTGGAAATGGGGGACAGACACCAAATCCGACGTTCC TCTTCCATCGCAACTTATATCTGTTGTCTGAAACAATAGGCTGCAGAAG TAAACCTCAATCGGATAGTAAAGACATATATAAAGTGACCCATTTATAT ATGTAAATTATATATATTCTCGCTTATGTATGGATTTACATAGGCACAT GTATGCTACACGTTACATATGCATATATGCATACAAACCTGATC
Zfhx4	chr2:119,024,967-119,025,086	TTTTGGAACAGCTGTAAATTAGTGATGAGCTATTAGTGAGCTGTGTCAT TATTTAATAAAAATGGCTTCTCTCACCTTATTTTTTATCCAGGTCCCTG ACAGGCTGGATGAAATGAGATCGATCTGCAAGGACTCGGAGTAGCTTAG GCTGTAATCAGGCTACTATTACAGTGGCTGGAGCCTTGCAGGCTCCCAA AAAAATGAAGGAAAGCAGACTTTTAACCAATGTGTGACCAACTT
aGlobin	chr14:12,097,459-12,097,578	GATCCTAACACTAACCCCAGCTCGCGTCGGGGTCCAACCCCCCCAGCCT GCGCAGTATCGTGGGTGGGGCAGGGCAGCAGCCCTGCCTGGCTGGGGTC CAGAATCTATGGGGCGGGCTGGACAAGAACAACGTCAAGGGCATCTTCA CCAAAATCGCCGGCCATGCTGAGGAGTATGGCGCCGAGACCCTGGAAAG GTAGGTGTCCTTCTCTGTCCTCCGGCTGCCTCTCTCCCCTGATC

Supp. table 2. Primer design for multiplex enhancer cloning and Nanostring screening. Related to figure 2.

	Primer sequence			
		BsmBI binding site	Vector specific overhangs	Target specific sequence (~20nt)
Cerulean vectors F	TTTTTT	CGTCTC	ccatgg	nnnnnnnnnnnnnnnnnnn
Cerulean vectors R	TTTTTT	CGTCTC	ggtcct	nnnnnnnnnnnnnnnnnnn
Citrine vectors F	TTTTTT	CGTCTC	gccagg	nnnnnnnnnnnnnnnnnnn
Citrine vectors R	TTTTTT	CGTCTC	caacag	nnnnnnnnnnnnnnnnnnn
Cherry vectors F	TTTTTT	CGTCTC	gtgcag	nnnnnnnnnnnnnnnnnnn
Cherry vectors R	TTTTTT	CGTCTC	caccgt	nnnnnnnnnnnnnnnnnnn
Cerulean neg control oligo F	TTTTTT	CGTCTC	ccatgg	AGCTGGATCGATgatatcCGATCGATCGTAGCAC
Cerulean neg control oligo R	TTTTTT	CGTCTC	ggtcct	GTGCTACGATCGATCGgatatcATCGATCCAGCT
Citrine neg control oligo F	TTTTTT	CGTCTC	gccagg	AGCTGGATCGATgatatcCGATCGATCGTAGCAC
Citrine neg control oligo R	TTTTTT	CGTCTC	caacag	GTGCTACGATCGATCGgatatcATCGATCCAGCT
Cherry neg control oligo F	TTTTTT	CGTCTC	gtgcag	AGCTGGATCGATgatatcCGATCGATCGTAGCAC
Cherry neg control oligo R	TTTTTT	CGTCTC	caccgt	GTGCTACGATCGATCGgatatcATCGATCCAGCT

Supp. table 3. Guide RNA sequences. Related to figures 4 and 6.

Epigenome engineering of *Sox10* enhancers		**Targeted knock-out of core TFs**	
Target/sgRNA	sgRNA sequence	Target/sgRNA	sgRNA sequence
84_sgRNA_1	AGTCTGCCACCCATCAAAGC	ATF2_sgRNA_1	TCAACAACTGAAACACCGGT
84_sgRNA_2	CCATTGTATCATGCTGGACA	ATF2_sgRNA_2	CTTGCTGTTTTCAGGCATCA
84_sgRNA_3	CTCCACTGAACGAGTCCATG	TFAp2b_sgRNA_1	GGAGGAGTGCTGAGAAGGTA
84_sgRNA_4	ATTAATTCCTGCGAACAGAA	TFAp2b_sgRNA_2	ACCCTCGCTTACCTTCCACC
84_sgRNA_5	CCCTTTGTGTATGGGCTCAC	Sox10_sgRNA_1	TTCCCTCCCCAGTGAGAAGA
85_sgRNA_1	AGATGTGCTTATGGGCTCCT	Sox10_sgRNA_2	GGTAGGAAAACTTACATTGC
85_sgRNA_2	TGGGAACAATGTCAACTCCG	Arnt2_sgRNA_1	AGGGACCCAGCAAATTTTCA
85_sgRNA_3	GCACAGAGCGGCCCCGTCG	Arnt2_sgRNA_2	TCTTTTGTTTATAGGTATGA
85_sgRNA_4	TTCAGTACAGCTACTTACAG	NR2C1_sgRNA_1	CTCTTTACCGCAGCGTATAC
85_sgRNA_5	TCTTTCCACCCGCCCAGGGC	NR2C1_sgRNA_2	AGACAACTCTCCCAATGAGC
87_sgRNA_1	CAGGAAGAAATGCGTAGTGA	Sox9_sgRNA_1	CTCTCATTCAGCAGCCTG
87_sgRNA_2	GAGCGAGCAGAGAGTGGAGC	NR2F2_sgRNA_1	CCAAAGGGTGAGAGAGGGAA
87_sgRNA_3	TCTTTGTTCCCTGCCTTTAA	NR2F2_sgRNA_2	GGCATGAGACGGGAAGGTAT
87_sgRNA_4	CTCTAAAACACCCGATTGTC	Otx2_sgRNA_1	CCAAAGGGTGAGAGAGGGAA
87_sgRNA_5	GCAGGGAAGGAGGATTCTGA	Otx2_sgRNA_2	CCAAAGGGTGAGAGAGGGAA
89_sgRNA_1	AGGGCATCCCCATGCACAAC	Pax2_sgRNA_1	CCAAAGGGTGAGAGAGGGAA
89_sgRNA_2	GAGGCAACAAATCTTTTCCA	Pax2_sgRNA_2	CCAAAGGGTGAGAGAGGGAA
89_sgRNA_3	AGGCAACTCACTGAGCATGA		
89_sgRNA_4	GGGGAGAGTAAATGAGACAG		
89_sgRNA_5	CAGTCAGTTGGGCTGCAGAG		
99_sgRNA_1	GGTGAGAAATGTTGAAAACG		